ORIGINAL ARTICLE

American Journal of of Orthodontics and Dentofacial Orthopedics. 128(1): 27-34, 2005.

Comparison of relative mandibular growth vectors with high-resolution 3-dimensional imaging

Lucia H. S. Cevidanes,[a*] Alexandre A. Franco,[b] Guido Gerig,[c] William R. Proffit,[d] Dennis E. Slice,[e] Donald H. Enlow,[f] Henrique M. Lederman,[g] Leila Amorim,[h] Marco A. Scanavini[i], and Julio W. Vigorito[j]

Chapel Hill and Winston-Salem, NC, São Paulo, Brazil, and Cleveland, Ohio

Introduction: The mandibular rami and their endochondrally growing condyles develop in many directions relative to the variable anatomic patterns of the nasomaxilla and middle cranial fossae during growth and response to orthopedic treatment. **Methods:** High-resolution magnetic resonance images were used to compare 3-dimensional (3D) growth vectors of skeletal displacement and bone remodeling in 25 untreated subjects with Class II malocclusions, 28 subjects with Class II malocclusions who were treated with Fränkel appliance therapy, and 25 subjects with normal occlusions. Marked differences were noted over an 18-month observation period. The 3D coordinates of anatomic landmarks were registered by Procrustes fit to control for rotation, translation, and scale differences. **Results:** Compared with untreated Class II and normal-occlusion subjects, the treated group showed highly significant differences in the 3D displacement/remodeling vectors of gonion and pterygomaxillary fissure relative to condylion and middle cranial fossae bilateral skeletal landmarks, by using both permutation tests ($P < .001$) and a general linear multivariate model ($P < .0001$). **Conclusions:** In a prospective and systematically controlled study, we quantitatively described significant 3D rami skeletal compensations in the structural assembly of facial morphogenesis at the beginning of the adolescent growth spurt using novel modeling techniques. These techniques have facilitated quantification of relative 3D growth vectors to illustrate skeletal changes with Fränkel appliance therapy. Future studies are required to assess the long-term clinical significance of our findings. (Am J Orthod Dentofacial Orthop 2005;128:27-34)

[a]Postdoctoral fellow, Department of Orthodontics, School of Dentistry, University of North Carolina, Chapel Hill.
[b]PhD program in Diagnostic Imaging, Paulista School of Medicine, UNIFESP, São Paulo, SP, Brazil.
[c]Taylor Grandy Professor of Computer Science and Psychiatry, University of North Carolina.
[d]Kenan Professor, Department of Orthodontics, University of North Carolina School of Dentistry.
[e]Assistant professor, Department of Biomedical Engineering, Wake Forest University School of Medicine, Winston-Salem, NC.
[f]Thomas Hill Emeritus Professor, Case Western Reserve University, Cleveland, Ohio.
[g]Professor, Department of Diagnostic Imaging Orthodontics, Paulista School of Medicine, UNIFESP, São Paulo, SP, Brazil.
[h]Research assistant, Department of Biostatistics, University of North Carolina.
[i]Professor and chairman, Department of Orthodontics, Methodist University of São Paulo, São Bernardo, SP, Brazil.
[j]Professor and chairman, Department of Orthodontics, University of São Paulo, São Paulo, SP, Brazil.

CNPq, a Brazilian governmental agency for scientific and technological development, scholarship 20005-98/7, supported work by L.H.S.C. FAPESP-Brazil grant 97/01388-8 supported work by A.A.F., J.W.V., H.K.Y., and M.A.S. UNC Dental Research Center supported work by L.A. and G.G. Work by D.E.S. was supported, in part, by the Austrian Ministry of Education, Science, and Culture, the Austrian Council for Science and Technology (grant number: AD 387/25-30 to Horst Seidler), Dr Edward G. Hill, and members of the Winston-Salem community.

Reprint requests to: Lucia H. S. Cevidanes, Department of Orthodontics, School of Dentistry, 201 Brauer Hall, University of North Carolina, CB#7450, Chapel Hill, NC 27599-7450; e-mail, cevidanl@dentistry.unc.edu.

Submitted, September 2003; revised and accepted, March 2004.
0889-5406/$30.00

doi:10.1016/j.ajodo.2004.03.033

Estimation of 3-dimensional (3D) displacement and bone remodeling is important for quantifying outcomes of orthopedic therapy and orthognathic surgery, and correcting craniofacial anomalies and developmental defects.[1] Although growth of the face and jaws has been measured in 2 dimensions, structural changes at specific locations are not sufficiently reflected in cephalometric measurements.[2-6] Three-dimensional quantitative assessment of morphologic alterations has the potential to precisely locate changes of clinical significance in craniofacial[1,4,6-9] or neurologic[10,11] disorders, identifying major features of the 3D growth vectors.[12]

During growth and response to orthopedic treatment, the mandibular rami and condyles develop in many directions relative to all possible individual variations in the nasomaxilla and middle cranial fossae anatomic patterns.[13-16] However, identification of the rami's role relative to skeletal compensations in maxillomandibular discrepancy corrections cannot be addressed by comparisons with population norms, angles, and interlandmark distances.[17,18] This prospective study used high-resolution 3D magnetic resonance images, applying mathematically sound and readily interpreted analytical methods. Magnetic resonance

imaging (MRI) has been applied for visualization and accurate measurement of skeletal and soft tissues.[19] Bookstein[20] and Dryden and Mardia[21] presented groundbreaking mathematical methods for 3D morphological analysis based on the coordinates of anatomical landmarks.

Evidence that the rami and the condyles might play compensatory roles in skeletal growth and response to treatment comes from the findings of implant[14,15] and histological[16] studies. Now, quantitative descriptors of 3D rami skeletal compensations can assess the manner of assembly of structural components involved in facial morphogenesis. The quantification of changes in skeletal morphology includes 2 significant developmental processes during bone growth: primary or secondary displacement, and bone surface remodeling.[16] The alteration of landmark position during growth and treatment involves these simultaneous processes of bone surface remodeling, primary displacement by individual bone growth, and secondary displacement by the growth of adjacent structures. This study assessed the 3D displacement/remodeling at skeletal landmarks between high-resolution MRIs taken initially (T1) and 18 $\pm$ 1 months later (T2) of children at the beginning of the adolescent growth spurt. Specifically, we quantified the structural change at skeletal landmarks in the mandibular rami relative to the middle cranial fossae and the posterior boundary of the nasomaxilla. This assessment included landmarks located at the rami boundaries and articulations with other anatomic components during growth, such as the pharyngeal space beneath the middle cranial fossae, between the right and left temporomandibular joints, and the posterior part of the maxilla that places the mandibular corpus and its dental arch in functional occlusion.

MATERIALS AND METHODS

This prospective study sample included 156 (2 x 78) MRI 3D head scans from 78 children (41 girls, 37 boys). The MRIs were taken at T1 and T2. A graduate student (A.A.F.) and an assistant professor (L.H.S.C.) at the Department of Orthodontics, Methodist University of São Paulo, Brazil, recruited and screened children in neighborhood schools and assessed them clinically. The inclusion criteria specified white Brazilian children aged 9 to 12 years, at the end of the mixed dentition, at the beginning of the pubertal growth spurt (evaluated by skeletal maturation in hand and wrist x-rays), with no early loss of primary teeth, and no absence of permanent teeth. Fifty-three patients who met these criteria had clinical evaluations of Class II Division 1 malocclusions, with at least three-fourths cusp Class II molars and overjets between 4.5 and 10 mm; 25 subjects had normal occlusions, with molar relationships of Class I or edge-to-edge, canines in Class I, and overjets from 1 to 2.5 mm.

The Class II subjects were randomly allocated to 2 subgroups, treated and control, to avoid bias in the group comparisons.[22] The treated group comprised 28 subjects treated with orthopedic appliances for mandibular advancement; the control group included 25 untreated subjects. The Class II controls received treatment after the 18-month observation period. The 25 children with normal occlusions served as a normal group for comparisons. At T1, the mean ages were 10.3 $\pm$ 0.9 years for the treated group, 10.9 $\pm$ 0.7 years for the Class II control group, and 10.2 $\pm$ 0.8 years for the normal group.

The clinical assessment and image acquisition and analysis protocols were described by previously by Cevidanes et al.[23,24]

This analysis included identification and recording of coordinates of 8 bilateral, 3D anatomic landmarks in the coronal, axial, and sagittal planes at craniofacial growth, remodeling, and displacement fields[13-16,25]: (1) maxillary tuberosity, (2) mandibular condyle, (3) posterior and lower borders of the rami, and (4) greater wings of the sphenoid.[24] The landmarks were analyzed as fully informative 3D locations, although future analyses could control for less-informative directions of variation.[24]

Statistical analysis

Two statistical approaches were used to assess 3D landmark relative displacement/remodeling from T1 to T2. The first approach was generalized least-squares Procrustes analysis (GPA)[20,21,26-29] of the 156 images of the landmark coordinate data sets. Permutation tests of the coordinate-wise differences between T1 and T2 for individual landmarks after superimposition determined whether the relative 3D displacement/remodeling with growth/response to treatment was differently distributed in the treated, untreated Class II, and normal-occlusion groups. The permutation tests were performed by using Morpheus et al.[30]

The second approach involved rotation, translation, and scaling of each T1 landmark coordinate data set by Procrustes fit relative to a template that was the average of 5 normal subjects not included in the sample. Each T2 landmark coordinate data set was rotated and translated with Procrustes fit applying the T1 scale factor of its matching configuration to control size variability without scaling the growth/treatment response changes. A general linear multivariate model (8.2, SAS, Cary, NC) was used to determine the coordinate-wise differences between T1 and T2 for each landmark. The saturated model was given by:

$Y_{(78 \times 24)} = X_{(78 \times 8)} B_{(8 \times 24)} + E_{(78 \times 24)}$, where Y denoted the matrix with columns being differences between T1 and T2 for the x, y, and z landmark coordinates of the right and left anatomical landmarks (condylion, gonion, middle cranial fossa, pterygomaxillary fissure) and with rows corresponding to subjects. These were considered within-subject variables. The rows $\{Y_i\}$ were considered mutually independent, with $\varepsilon Y = XB$, while the landmark displacement/remodeling within a person was correlated. X was the "design matrix," which was assumed to be fixed and known, or at least conditional on choosing the sampling units. In this case, the predictors in the model (between-subject effects) were sex and group (treated, untreated Class II, and normal occlusion). So, $X = [1\ X_1\ X_2\ X_3\ X_4\ X_5\ X_6\ X_7]$, where X_1 represented the vector (78 x 1) that contains the sex of the subject, X_2 the centered age, X_3 the quadratic centered age, X_4 the group, X_5 the interaction between group and sex, X_6 the interaction between centered age and group, and X_7 the interaction between quadratic centered age and group. B was the matrix regression coefficients that were unknown, so that:

$$B = \mu_{o,1}\ \mu_{o,2} \cdots \mu_{o,24}$$
$$\mu_{M,1}\ \mu_{M,2} \cdots \mu_{M,24}$$
$$\mu_{agec,1}\ \mu_{agec,2} \cdots \mu_{agec,24}$$
$$\cdots\cdots\cdots$$
$$\mu_{gr,age2,1}\ \mu_{gr,age2,2} \cdots \mu_{gr\_age2,24(8\times24)}$$

In this case, we considered each row iid, such that: $row_i(E) \sim N_{78}(0, \Sigma_{(78 \times 78)})$

Because the 3 groups did not show significant interactions with sex, quadratic centered age, and centered age, these terms were removed from the investigation model. We used the mean between right and left landmark coordinates as the outcome response, because no effect of landmark side (right or left) in the group was observed, and this sample did not have noticeable asymmetry. Because right and left displacement/remodeling would be geometrical mirrors, the data were coded with respect to anteroposterior, inferosuperior, and lateromedial directions of displacement/remodeling. Hence, the final model includes 12 response variables (right/left averages) and only the treatment group as the factor for the landmark displacement/remodeling between T1 and T2. To access statistical significance, we used the Wilks test at the 5% level of significance and the Bonferroni adjustment when it involved multiple pairwise comparisons,[31] where all the P values reported refer to the mean value of the scaled displacement/remodeling between T1 and T2. For quantitative assessment of relative landmark displacement/remodeling, the scale factor was put back into the analysis, the data were rescaled by the original T1 scale factors, and descriptive statistics of median values and quartiles were reported in millimeters.

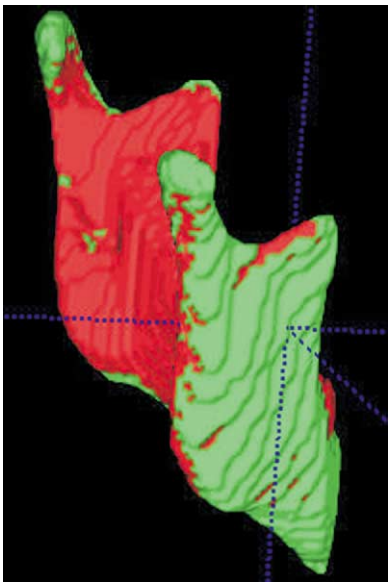

Fig 1. Overlap of mandibular ramus at T1 (*red*) and T2 (*green*). Mandibular rami 3D models are shown without surface smoothing but, rather, display exact segmentation of each 1-mm thick slice.

RESULTS

The Procrustes fit based on 3D landmark pairs, located at the boundaries of anatomic components that articulate during growth, allowed relative superimposition of the mandibular rami at T1 and T2, as shown in Figure 1. The relative surface distance between T1 and T2 structures can indicate the growth/response to treatment alterations as a result of either remodeling or displacement. In Figure 2, *blue* suggests areas of bone resorption or displacement, and *red* suggests areas of potential bone deposition or displacement.

Generalized least-squares Procrustes analysis of the 156 landmark-coordinate data sets removed variability among different image acquisitions because of rotation, translation, and size that could overwhelm and obscure variability in craniofacial form (Fig 3). When we compared the treated group with the untreated control group with Class II malocclusions and normal-occlusion groups (Table), permutation tests of the net difference between T1 and T2 for each landmark showed highly significant differences of the 3D relative displacement/remodeling vectors of gonion and pterygomaxillary fissure bilateral skeletal landmarks ($P < .001$, Bonferroni adjusted), and significant differences

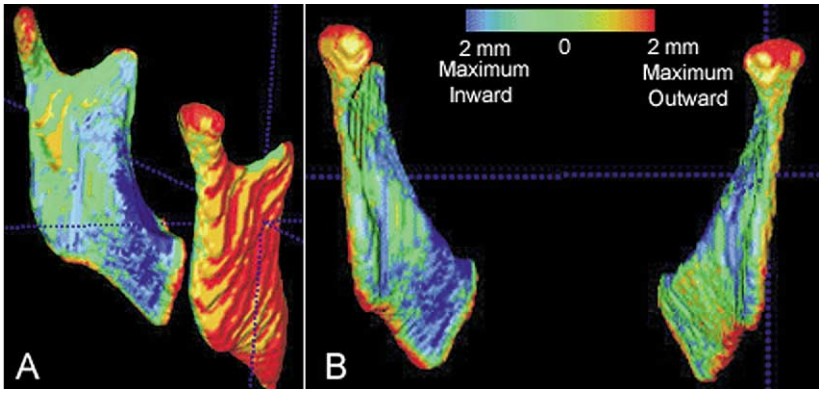

Fig 2. Surface distance between T1 and T2 images with color coding: *blue* indicates inward movement or bone resorption to *red*, indicating outward movement or bone deposition. **A**, Lateral view of mandibular rami; **B,** posterior view.

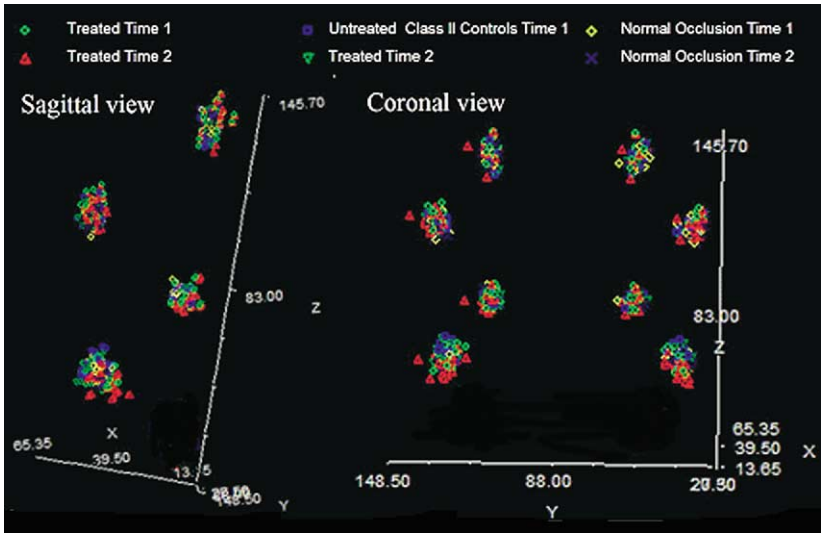

Fig 3. Generalized least-squares Procrustes fit of 156 landmark-coordinate data sets.

Table. Permutation tests of landmarks' overall 3D displacement/remodeling between T1 and T2

Group	*Co*	*Go*	*MCF*	*PTM*
Treated vs normal occlusion	0.323	0.001*	0.001*	0.001*
Treated vs untreated Class II controls	0.103	0.001*	0.073	0.001*
Normal occlusion vs untreated Class II controls	0.180	0.595	0.055	0.328

Co, Condylion; *Go*, gonion; *MCF,* middle cranial fossa; *PTM*, pterygomaxillary fissure.
*Statistically significant.

in the relative displacement/remodeling of the middle cranial fossae landmarks between the treated and normal-occlusion groups.

The assessment of coordinate-wise landmark displacement/remodeling relative to the other landmarks included in the Procrustes registration showed the 3D vectors of growth/response to treatment and quantified the relative landmark displacement/remodeling in the 3 planes of space (Figs 4 to 7).

Relative to the mandibular and middle cranial fossa landmarks, the median of pterygomaxillary fissure landmark displacement/remodeling in the treated group was 1 mm in a posterior direction (Fig 4). The multivariate tests of the mean scaled displacement/remodeling showed $P < .0001$ when the treated group was compared with the normal-occlusion and untreated Class II groups.

Relative gonion landmark displacement/remodeling

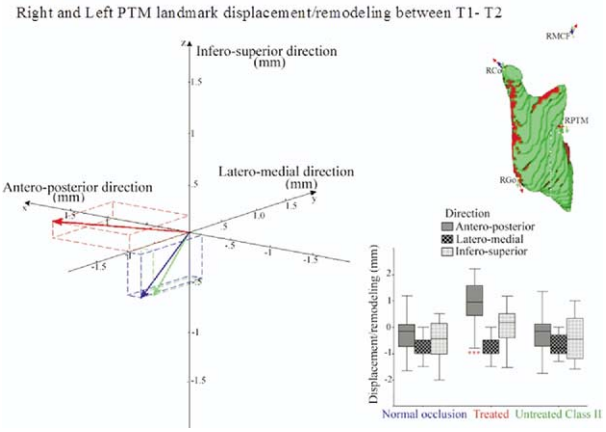

Fig 4. 3D vectors of median values of relative pterygomaxillary fissure landmark displacement/ remodeling for each group. *Red asterisks* in boxplot indicate signifiant T1-T2 changes in relative posterior direction when treated group was compared with normal-occlusion and untreated Class II groups.

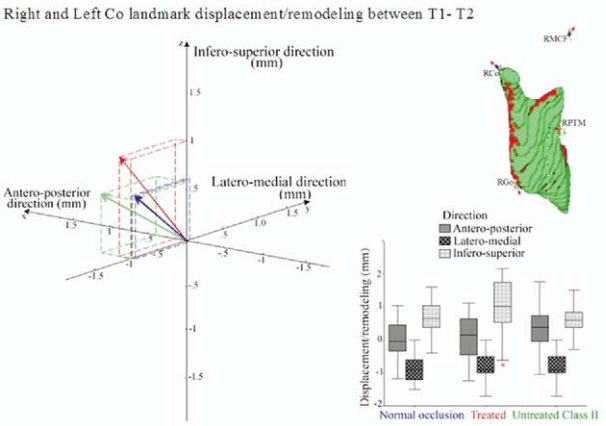

Fig 6. 3D vectors of median values of relative condylion landmark displacement/remodeling for each group. *Red asterisks* in boxplot indicate statistical significance in T1-T2 changes in relative superior direction when treated group was compared with untreated Class II group.

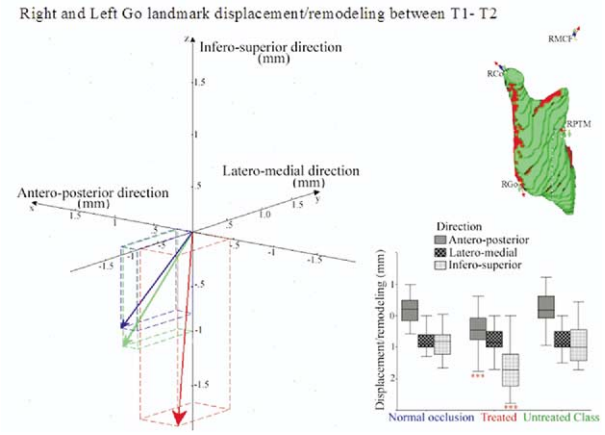

Fig 5. 3D vectors of median values of relative gonion landmark displacement/remodeling for each group. *Red asterisks* in boxplot indicate significant T1-T2 changes in relative anterior and inferior direction when treated group was compared with normal-occlusion and untreated Class II groups.

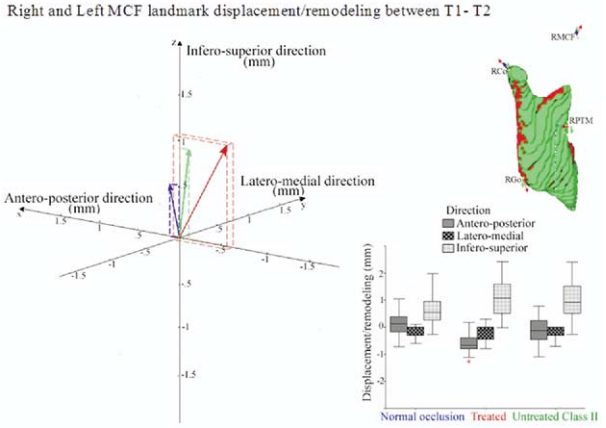

Fig 7. 3D vectors of median values of relative middle cranial fossae landmark displacement/remodeling for each group. *Red asterisks* in boxplot indicate statistical significance in relative anterior displacement/remodeling between T1 and T2 when treated group was compared with normal-occlusion group.

in the treated group was highly significant when compared with the normal occlusion (mean scaled displacement/remodeling P value $<.0001$) and untreated Class II groups (mean scaled displacement/remodeling with P value $< .0001$) in both the anterior direction (median value, -0.46 mm) and the inferior direction (median value, -1.72 mm, Fig 5).

The vertical component of the 3D vector of relative condylion landmark displacement/remodeling (median value, 1.02 superior direction) was significantly different when the treated group was compared with the untreated Class II controls ($P = .007$). The condylion landmarks showed relative displacement/remodeling in the opposite directions of the gonion landmarks displacement/remodeling in all groups (Fig 6).

A statistically significant difference in displacement/remodeling of the middle cranial fossae landmark displacement/remodeling in the treated group compared with the normal-occlusion group was observed in both the permutation tests ($P < .001$) and the general

linear multivariate model ($P < .0001$) for the anterior component of the displacement/remodeling vector), despite the small median value difference (−.038 mm) (Fig 7).

DISCUSSION

The displacement/remodeling at 3D skeletal landmarks during growth and response to treatment was assessed by using generalizable methods for identification of structural changes at specific locations that reflect the assembly of structural components in facial morphogenesis. Quantifying landmark displacement/remodeling is difficult not only because of registration and homology issues[20] but also because the choice of landmark locations spans different structural components of the face,[32] with diverse timing and patterns of skeletal growth processes.[33]

This study was the first to attempt to quantify relative landmark displacement/remodeling of key counterpart components of the face in a prospective 3D investigation. Mandibular rami growth occurs relative to its counterparts, the middle cranial fossae and the posterior nasomaxilla, which are established earlier in craniofacial morphogenesis.[17] McIntyre and Mossey[34] evaluated the clinical relevance of current geometric morphometric tools compared with conventional cephalometrics. In our study, Procrustes analysis was applied for T1 to T2 comparisons of landmark displacement/remodeling relative to the other landmarks included in the 3D models. The Procrustes technique scale was put back into the analysis to report the actual size alterations of the rami. Rohlf[35,36] has shown that the Procrustes method is the most powerful approach to measuring mean shape differences in configurations of landmarks, while controlling for differences in the configurations that could be due to the effects of rotation, translation, and scale. Linear distance-based methods strongly constrain the possible results obtained and can give misleading results when used in studies of growth and evolutionary trajectories.[36,37] Although finite element analysis[38-41] can in theory be applied for modeling physical deformation during growth of anatomical structures, it requires subdividing the landmarks located on an object into groups to form the finite elements. A general homology function that arbitrarily maps the locations of mathematically homologous points internal to each finite element in the initial form[42] does not appear to be useful for studying key components in the biologic processes of craniofacial morphogenesis.[17] However, the vectors of the T1 to T2 Procrustes distances appear effective in recognizing the 3D growth directions of skeletal landmark displacement/remodeling relative to their developmental counterparts. Such a method that takes into account the relative displacement/remodeling of structural components appears to be the most effective in recognizing alterations in the configuration of the facial skeletal structures, characterized by remodeling processes in many directions that shape and enlarge the bones to match the distribution, functioning, and enlargement of all facial soft tissues and organs.[13,25] Some important points should be made about our methods, however. First, the spatial resolution might affect the accuracy of the findings of the imaging technique.[10,43-45] We therefore controlled the acquisition protocol for all images to be taken with a high spatial resolution of 1 x 1 x 1 mm isotropic voxels.[24]

A second point is that the number of landmarks assessed in this study limits our information about the facial structures' relative locations.[20] The criteria for landmark choice included landmarks at maximal surface curvature of skeletal growth sites, not affected by dental movement, and distributed among the mandibular rami and their anatomical counterparts. Although this approach might ultimately be superseded by others, such as analysis of the whole curves[46,47] of the condyles and rami contour relative to the curves of the maxillary, sphenoid, and temporal bone boundaries, it was the safest approach under conditions in which many growth directions often require the simplification of parameters to about 20 to 30 to obtain a more compact and easy-to-understand representation.[47] This is an active area of research that can ultimately help this project.

Our methods describe relative, not absolute, landmark displacement/remodeling.[20,42] This study assessed compensatory changes in skeletal counterpart components of the face during treatment of Class II malocclusion, evaluating the differential 3D growth vector directions of 4 bilateral landmarks. The lateral growth of the face, as described by the 3D growth vectors, did not show statistically significant differences when we compared the treated, untreated control with Class II malocclusion, and normal-occlusion groups. The highly significant anterior displacement/remodeling of gonion landmarks in the treated group compared with the normal-occlusion and untreated Class II groups occurred in the opposite direction of the highly significant relative posterior component of the 3D displacement/remodeling vector of the pterygomaxillary fissure landmarks; this suggests skeletal correction of the maxillomandibular discrepancy in Class II malocclusions. The relative anterior displacement/remodeling of gonion landmarks also occurred in the opposite direction of condylion landmarks, describing the alteration in rami alignment relative to the middle

cranial fossae and pterygomaxillary fissure landmarks in the treated group. The highly significant inferior direction of gonion displacement/remodeling in the treated group compared with the normal-occlusion and untreated Class II groups was observed relative to a significant superior displacement/remodeling of condylion landmarks when the treated group was compared with the untreated Class II controls. These findings characterize the vertical growth/response to treatment of the mandibular ramus relative to the composite vertical dimension of the posterior part of the nasomaxilla and middle cranial fossae. The middle cranial fossae landmark displacement/remodeling in the treated compared with the normal-occlusion group was statistically significant but small. Hence, the 18-month Fränkel appliance therapy at the beginning of the adolescent growth spurt promoted highly significant statistical differences in the 3D mandibular rami growth relative to its counterparts; this corroborates our findings with a 2-dimensional counterpart analysis.[23] The relatively small magnitude of the 3D growth vectors might explain why they are often missed with conventional cephalometrics.[48]

CONCLUSIONS

The growth vectors of landmark displacement/remodeling are only 1 of several measures of 3D skeletal alterations that clinicians can use. The assessment of patterns of mandibular growth remodeling, with analyses of skeletal and dental compensations, can clarify whether it makes a difference to treat the maxilla or the mandible. Determining such patterns, in combination with 3D vectors of growth displacement/remodeling, provides a new, exciting means of quantitative image analysis that can be helpful in diagnosing and evaluating various maxillomandibular discrepancies.

Three-dimensional vectors of gonion and pterygomaxillary fissure displacement/remodeling relative to condylion and middle cranial fossae bilateral skeletal landmarks quantified skeletal changes in the facial morphogenesis. These skeletal changes were relatively more forward and vertically increased rami in the treated compared with the control group. This methodology is generalizable and can be applied to other imaging modalities.

We thank Dr Fred L. Bookstein for his invaluable assistance in the multivariate aspects of this work and Dr Kurt Faltin, Jr, for his contribution and discussions in the clinical assessment of the Fränkel appliance.

REFERENCES

1. Hennessy RJ, Moss JP. Facial growth: separating shape from size. Eur J Orthod 2001;23:275-85.
2. Ghafari J, Baumrind S, Efstratiadis SS. Misinterpreting growth and treatment outcome from serial cephalographs. Clin Orthod Res 1998;1:102-6.
3. Harrell WE Jr, Hatcher DC, Bolt RL. In search of anatomic truth: 3-dimensional digital modeling and the future of orthodontics. Am J Orthod Dentofacial Orthop 2002;122:325-30.
4. Togashi K, Kitaura H, Yonetsu K, Yoshida N, Nakamura T. Tri-dimensional cephalometry using helical computer tomography: masurement error caused by head inclination. Angle Orthod 2002;72:513-20.
5. Tulloch JFC, Medland W, Tuncay OC. Methods used to evaluate growth modification in Class II malocclusion. Am J Orthod Dentofacial Orthop 1990;98:340-7.
6. Turpin DL. Research topics—past, present, and future. Am J Orthod Dentofacial Orthop 2002;122:341.
7. Baumrind S, Moffitt FH, Curry S. The geometry of three-dimensional measurement from paired coplanar x-ray images. Am J Orthod 1983;84:313-22.
8. Kusnoto B, Evans CA. Reliability of a 3D surface laser scanner for orthodontic applications. Am J Orthod Dentofacial Orthop 2002;122:342-8.
9. Troulis MJ, Everett P, Seldin EB, Kikinis R, Kaban LB. Development of a three-dimensional treatment planning system based on computed tomographic data. Int J Oral Maxillofac Surg 2002;31:349-57.
10. Bullitt E, Gerig G, Pizer SM. Aylward SR. Measuring tortuosity intracerebral vasculature from MRA images. IEEE Trans Med Imaging 2003;22;1163-71.
11. Styner M, Gerig G, Lieberman J, Jones D, Weinberger D. Boundary and medial shape analysis of the hippocampus in schizophrenia. Med Image Anal 2004;8:197-203.
12. Williams AL, Jeffery G. Growth dynamics of the developing lateral geniculate nucleus. J Comp Neurol 2001;430:332-42.
13. Bhat M, Enlow DH. Facial variations related to headform type. Angle Orthod 1985;55:269-80.
14. Björk A, Skieller V. Contrasting mandibular growth and facial development in long face syndrome, juvenile rheumatoid polyarthritis, and mandibulofacial dysostosis. J Craniofac Genet Dev Biol (Suppl)1985;1:127-38.
15. Björk A, Skieller V. Normal and abnormal growth of the mandible. A synthesis of longitudinal cephalometric implant studies over a period of 25 years. Eur J Orthod 1983; 5:1-46.
16. Petrovic A, Stutzmann J, Lavergne J. Mechanism of craniofacial growth and modus operandi of functional appliances: a cell-level and cybernetic approach to orthodontic decision making. In: Carlson DS, editor. Craniofacial growth theory and orthodontic treatment. Monograph 23. Craniofacial Growth Series. Ann Arbor: Center for Human Growth and Development; University of Michigan; 1990. p. 13-74.
17. Enlow DH, Kuroda T, Lewis AB. Intrinsic craniofacial compensations. Angle Orthod 1971;41:271-85.
18. Moyers RE, Bookstein FL. The inappropriateness of conventional cephalometrics. Am J Orthod 1979;75:599-617.
19. Arens R, McDonough JM, Corbi AM, Rubin NK. Carroll ME, Pack AI, et al. Upper airway size analysis by magnetic resonance imaging of children with obstructive sleep apnea syndrome. Am J Respir Crit Care Med 2003;167:65-70.
20. Bookstein FL. Shape and the information in medical Images: a decade of the morphometric synthesis. Comput Vis Image Understanding 1997;66:97-118.

21. Dryden IL, Mardia KV. Statistical shape analysis. New York: John Wiley & Son; 1998.
22. Phillips C, Tulloch C. The randomized clinical trial as a powerful means for understanding treatment efficacy. Sem Orthod 1995; 1:128-38.
23. Cevidanes LHS, Franco AA, Scanavini MA, Enlow DH, Vigorito JW, Proffit WR. Clinical outcomes of Fränkel appliance therapy assessed with counterpart analysis. Am J Orthod Dentofacial Orthop 2003;123:379-87.
24. Cevidanes LHS, Franco AA, Gerig G, Proffit. WR, Slice DE, Enlow DH, et al. Assessment of mandibular growth and response to orthopedic therapy with 3-dimensional magnetic resonance images. Am J Orthod Dentofacial Orthop 2005; **in press**.
25. Enlow DH, Kuroda T, Lewis AB. The morphologic and morphogenetic basis for craniofacial form and pattern. Angle Orthod 1971;41:161-88.
26. Bookstein FL, Sampson PD, Streissguth AP, Connor PD. Geometric morphometrics of corpus callosum and subcortical structures in the fetal-alcohol-affected brain. Teratology 2001;64:4-32.
27. Bookstein FL, Schafer K, Prossinger H, Seidler H, Fieder M, Stringer C, et al. Comparing frontal cranial profiles in archaic and modern homo by morphometric analysis. Anat Rec 1999; 257:217-24.
28. Bookstein FL, Streissguth AP, Sampson PD, Connor PD, Barr HM. Corpus callosum shape and neuropsychological deficits in adult males with heavy fetal alcohol exposure. Neuro Image 2002;15:233-51.
29. Gharaibeh WS, Rohlf FJ, Slice DE, DeLisi LE. A geometric morphometric assessment of change in midline brain structural shape following a first episode of schizophrenia. Biol Psychiatry 2000;48:398-405.
30. Slice DE. Morpheus et al: software for morphometric research. Revision 1-30-98. Stony Brook (NY): State University of New York, Department of Ecology and Evolution; 1998. (Recent beta).
31. Muller KE, Fetterman BA. Regression and ANOVA: an integrated approach using SAS software. Cary (NC): SAS Institute; 2002.
32. Adams DC. Methods for shape analysis of landmark data from articulated structures. Evol Ecol Res 1999;1:959-70.
33. Proffit W. Contemporary orthodontics. 3rd ed. Saint Louis: Mosby; 2000. p. 742.
34. McIntyre GT, Mossey PA. Size and shape measurement in contemporary cephalometrics. Eur J Orthod 2003;25:231-42.
35. Rohlf FJ. On the use of shape spaces to compare morphometric methods. Hystrix 2000:11:9-25.
36. Rohlf FJ. Statistical power comparisons among alternative morphometric methods. Am J Phys Anthropol 2000;111:463-78.
37. Slice DE. Landmark coordinates aligned by Procrustes analysis do not lie in Kendall's shape space. Syst Biol 2001;50:141-9.
38. Cattaneo PM, Dalstra M, Melsen B. The transfer of occlusal forces through the maxillary molars: a finite element study. Am J Orthod Dentofacial Orthop 2003;123:367-73.
39. Melsen B, Dalstra M. Distal molar movement with Kloehn headgear: is it stable? Am J Orthod Dentofacial Orthop 2003; 123:374-8.
40. Singh GD, Clark WJ. Localization of mandibular changes in patients with Class II Division 1 malocclusions treated with Twin-block appliances: finite element scaling analysis. Am J Orthod Dentofacial Orthop 2001;119:419-25.
41. Singh, GD, McNamara JA, Lozanoff S. Mandibular morphology in subjects with Class III malocclusions: finite-element morphometry. Angle Orthod 1998;68:409-18.
42. Richtsmeier JT, Deleon VB, Lele SR. The promise of geometric morphometrics. Yearbook Phys Anthropol 2002;45:63-91.
43. May A, Ashburner J, Buchel C, McGonigle DJ, Friston KJ, Frackowiak RS, et al. Correlation between structural and functional changes in brain in an idiopathic headache syndrome. Nat Med 1999;5:836-8.
44. Disler DG, Marr DS, Rosenthal DI. Accuracy of volume measurements of computer tomography and magnetic resonance imaging phantoms by three-dimensional reconstruction and preliminary clinical application. Invest Radiol 1994;29:739-45.
45. Hoad CL, Martel AL, Kerslake R, Grevitt M. A 3D MRI sequence for computer assisted surgery of the lumbar spine. Phys Med Biol 2001;46:N213-20.
46. Andresen R, Bookstein FL, Conradsen K, Ersboll BK, Marsh JL, Kreiborg S. Surface-bounded growth modeling applied to human mandibles. IEEE Trans Med Imaging 2000;19:1053-63.
47. Subsol G, Thirion JP, Ayache N. A scheme for automatically building three-dimensional morphometric anatomic atlases: application to skull atlas. Med Image Anal 1998;2:37-60.
48. Chen JY, Will LA, Niederman R. Analysis of efficacy of functional appliances on mandibular growth. Am J Orthod Dentofacial Orthop 2002;122:470-6.